



LAWRENCE
LIVERMORE
NATIONAL
LABORATORY

Integrated Surface-groundwater Flow Modeling: a Free-surface Overland Flow Boundary Condition in a Parallel Groundwater Flow Model

S. J. Kollet, R. M. Maxwell

April 18, 2005

Advances in Water Resources

Disclaimer

This document was prepared as an account of work sponsored by an agency of the United States Government. Neither the United States Government nor the University of California nor any of their employees, makes any warranty, express or implied, or assumes any legal liability or responsibility for the accuracy, completeness, or usefulness of any information, apparatus, product, or process disclosed, or represents that its use would not infringe privately owned rights. Reference herein to any specific commercial product, process, or service by trade name, trademark, manufacturer, or otherwise, does not necessarily constitute or imply its endorsement, recommendation, or favoring by the United States Government or the University of California. The views and opinions of authors expressed herein do not necessarily state or reflect those of the United States Government or the University of California, and shall not be used for advertising or product endorsement purposes.

Integrated surface-groundwater flow modeling: a free-surface overland flow boundary condition in a parallel groundwater flow model

Stefan J. Kollet and Reed M. Maxwell

Environmental Science Division, Lawrence Livermore National Laboratory (L-208), 7000 East Avenue, Livermore, CA 94550 USA, E-mail: kollet2@llnl.gov, Phone: 925-422-9297, Fax: 925-422-3118

Abstract

Interactions between surface and ground water are a key component of the hydrologic budget on the watershed scale. Models that honor these interactions are commonly based on the conductance concept that presumes a distinct interface at the land surface, separating the surface from the subsurface domain. These types of models link the subsurface and surface domains via an exchange flux that depends upon the magnitude and direction of the hydraulic gradient across the interface and a proportionality constant (a measure of the hydraulic connectivity). Because experimental evidence of such a distinct interface is often lacking in field systems, there is a need for a more general coupled modeling approach.

A more general coupled model is presented that incorporates a new two-dimensional overland flow simulator into the parallel three-dimensional variable saturated subsurface flow code ParFlow. In ParFlow, the overland flow simulator takes the form of an upper boundary condition and is, thus, fully integrated without relying on the conductance concept. Another important advantage of this approach is the efficient parallelism incorporated into ParFlow, which is efficiently exploited by the overland flow simulator.

Several verification and simulation examples are presented that focus on the two main processes of runoff production : excess infiltration and saturation. The model is shown to reproduce an analytical solution for overland flow and compares favorably to other commonly used hydrologic models. The influence of heterogeneity of the shallow subsurface on overland flow is also examined. The results show the uncertainty in overland flow predictions due to subsurface heterogeneity and demonstrate the usefulness of our approach. Both the overland flow component and the coupled model are evaluated in a parallel scaling study and show to be efficient.

1 Introduction

The subsurface and surface are complex environmental systems that often behave in a coupled manner. Surface water in rivers, streams, lakes and wetlands is in constant communication with the vadose zone, shallow and deep groundwater systems. Thus, surface-groundwater interactions are an intrinsic component of the hydrologic budget on the watershed scale and hydrologic modeling tools must account for this interaction to provide reliable predictions. Surface-groundwater interactions have been a widely recognized research area by several scientific communities interested in different spatial scales varying from bedform scale in hyporheic exchange modeling to continental scale hydrologic response modeling.

The occurrence of surface water and its spatial and temporal distribution depends on climatic factors (e.g., amount and distribution of rainfall and temperature), vegetation, topography (micro and macro), and on the exchange of water between the surface and the sub-surface. The rate and direction of exchange (groundwater discharge at the land surface or surface water infiltration into the subsurface) depend on the rainfall rate, direction of the hydraulic gradient and hydraulic characteristics of the land surface.

The two major processes of runoff production are commonly referred to as Hortonian and Dunne runoff. Hortonian runoff, often referred to as excess infiltration, occurs when the rainfall rate exceeds the saturated hydraulic conductivity of the land surface. Under excess infiltration conditions, ponding (accumulation of water at the surface) can occur before the subsurface becomes entirely saturated (Kutilek and Nielsen, 1994). Dunne runoff, often referred to as excess saturation, occurs when the

rainfall rate is smaller or equal to the saturated hydraulic conductivity of the land surface. Under excess saturation conditions, ponding can occur only when the entire soil column becomes completely saturated and water exfiltrates at the surface (Kutilek and Nielsen, 1994). Although these two processes are often considered independent, in the presence of a non-uniform distribution of soil properties, infiltration and saturation excess are interrelated and may occur simultaneously at various spatial and temporal scales.

Traditionally, the coupling of the surface and subsurface domains has been done via a so-called exchange flux that appears in both the groundwater and surface water flow equations as general sink/source terms. In this approach, the exchange rate is expressed in terms of the conductance concept which assumes an interface connecting the two domains (e.g., Anderson and Woessner 1992; VanderKwaak and Loague, 2001). This interface is commonly characterized by a proportionality constant representing the connectivity between the surface and sub-surface and generally involves the ratio of the interface hydraulic conductivity and effective thickness (e.g., Hantush, 1965). Recent studies have included additional processes into the conductance concept to account for the influence of microtopography on surface saturation (VanderKwaak and Loague, 2001; Panday and Huyakorn, 2004). In many cases, the application of the conductance concept to real systems is problematic, because the existence of a distinct interface has yet to be demonstrated in the field (Kollet and Zlotnik, 2003; Cardenas and Zlotnik, 2003).

Numerical algorithms for solving the problem of variable saturated groundwater flow are widely available and have been published extensively (e.g., Huyakorn et al., 1986; Kirkland et al., 1992; Forsyth et al., 1995; Therrien and Sudicky, 1996; Miller et al., 1998; Jones and Woodward, 2001).

Overland flow simulators have been also studied extensively, though major problems with inappropriate stability criteria remain to be a problem in many cases (Taylor et al., 1974; Gottardi and Ventulli, 1993; Fiedler and Ramirez, 2000; Jaber and Mohtar, 2003). The coupling of surface and subsurface flow also received considerable attention recently, with most models coupled in a linked fashion, iterating over the exchange flux until some convergence criterion is reached. This approach may cause large mass balance errors (e.g., LaBolle et al., 2003) and numerical instabilities, because of the large differences in the time scales of the two processes (surface runoff occurring on a much shorter time scale than the subsurface). Previous studies are summarized briefly below.

Freeze and Harlan (1969) provided the first comprehensive conceptual and theoretical framework of an integrated hydrologic response model on the watershed scale. Later, Govindaraju and Kavvas (1991) developed a coupled model that accounts for 1D channel and overland flow and 3D variable saturated groundwater flow. They studied the response of variable source areas (saturated areas adjacent to the stream) to hydrologic and topographic variations. Woolhiser et al. (1996) studied the effect of subsurface heterogeneity in the hydraulic conductivity using an overland flow model coupled to the Smith-Parlange infiltration model. They demonstrated the effect of heterogeneity on the hydrograph and presented a technique that accounted for the influence of microtopography. Wallach et al. (1997) studied the error in the exchange rate between the surface and the subsurface when the exchange rate is calculated assuming zero ponding depth. Fiedler and Ramirez (2000) solved the 2D hydrodynamic flow equations using MacCormack finite differences. In their model, interactive infiltration is simulated using the Green-Ampt formulation. Gunduz and Aral (2004) solve the problem of coupled groundwater and 1D channel flow by forming a single matrix instead of solving two separate matrices for the two domains. Braunschweig et al. (2004) presented an integrated hydrologic modeling system that

incorporates routing of water inside channels and on the land surface coupled to infiltration processes. Putti and Paniconi (2004) discussed numerical issues, such as the influence of the time step size on the global convergence behavior, in coupling a 3D variable saturated flow model with a 1D diffusion formulation of the overland flow equations. VanderKwaak and Loague (2001) and Panday and Huyakorn (2004) presented fully coupled approaches including land surface processes, such as evaporation, and demonstrated their usefulness. A common theme among previous work summarized here is that these models rely on some form of the conductance concept. The current work presented in this paper differs from these studies in that it provides a framework for a more general approach.

This study presents a general framework for coupling the surface and groundwater flow equations, which does not rely on the conductance concept. The surface water equations are used to close the initial value problem of variable saturated groundwater flow, which results in an overland flow boundary condition. This overland flow boundary condition, which has not been published before in the presented form to our knowledge, takes into account the free surface of water ponded at the land surface. To demonstrate the usefulness of this approach, we developed a two-dimensional distributed overland flow simulator, which was implemented into the three-dimensional, variable saturated groundwater flow code ParFlow . We present verification and simulation examples that focus on the surface water component independently and the aforementioned processes of excess infiltration and saturation. We introduce subsurface heterogeneity in the hydraulic conductivity tensor resulting in surface runoff and hydrograph uncertainty. ParFlow was designed for parallel computer systems and has been used extensively in large-scale and high resolution modeling (Ashby and Falgout, 1996; Jones and Woodward, 2001). The overland flow simulator exploits ParFlow's parallel infrastructure effectively and is also fully parallel, which is demonstrated in a parallel efficiency study.

2 Theory

As mentioned in the Section 1, the theory of coupled surface-water groundwater systems has been the subject of many previous studies. Hence, the governing equations of overland flow and variable saturated groundwater flow have been discussed in great detail in the literature. We therefore, provide only a brief summary of these equations that form the basis for the set of coupled equations presented later in Section 2.5.

2.1 Shallow Overland Flow

In two spatial dimensions, the continuity equation can be written as

$$\frac{\partial \psi_s}{\partial t} = \nabla \bar{v} \psi_s - q_r(x) - q_e(x) \quad (1)$$

where \bar{v} is the depth averaged velocity vector [LT^{-1}]; ψ_s is the surface ponding depth [L], $q_r(x)$ is the rainfall rate [LT^{-1}] and $q_e(x)$ is the exchange rate with the subsurface [L], which will be discussed in detail below. Note, that in Equation (1) the flow depth is vertically averaged. Thus, vertical change of momentum in the column of ponded water is neglected in this formulation. This has been shown to be a good approximation for shallow systems.

If diffusion terms are neglected the momentum equation can be written as

$$S_{f,i} = S_{o,i} \quad (2)$$

which is commonly referred to as the kinematic wave approximation. In Eq 2 $S_{o,i}$ is the bed slope (gravity forcing term) [-], which is equal to the friction slope $S_{f,i}$ [L]; i stands for the x - and y -direction. Although we consider the kinematic wave in the current work, this formulation can be expanded to incorporate the diffusive and dynamic wave equations (Fiedler and Ramirez, 2000) .

Manning's equation is used to establish a flow depth-discharge relationship

$$v_x = -\frac{\sqrt{S_{f,x}}}{n} \psi_s^{2/3} \text{ and } v_y = \frac{\sqrt{S_{f,y}}}{n} \psi_s^{2/3} \quad (3)$$

where n [$\text{TL}^{-2/3}$] is the Manning's coefficient. This empirical relationship has been widely applied to describe surface water systems. Anisotropy in the Manning's coefficient is not considered here, though it could easily be incorporated.

At the outlet, two types of boundary conditions were implemented into the overland flow simulator: the gradient and critical depth outlet conditions (Equations 4 and 5, respectively)

$$q_{out} = \frac{\sqrt{S_{f,outlet}}}{n_{outlet}} \psi_{s,outlet}^{5/3} \quad (4)$$

$$q_{out} = \sqrt{g \psi_{s,outlet}^3} \quad (5)$$

where g is the acceleration due to gravity [L/T^2]. The gradient outlet condition is equivalent to the zero depth gradient condition of Panday and Huyakorn (2004) for the case of the diffusive wave approximation. The critical depth boundary condition results in a constant flow depth at the outlet.

2.2 Variable Saturated Groundwater Flow

The equation for variable saturated groundwater flow is the well-known Richards' equation

$$S_s S_w \frac{\partial \psi_p}{\partial t} + \phi \frac{\partial S_w(\psi_p)}{\partial t} = \nabla \cdot q + q_s + \frac{q_e}{m'} \quad (6)$$

$$q = -k(x) k_r(\psi_p) \nabla(\psi_p - z)$$

where ψ_p is the subsurface pressure head [L], z is depth below the surface [L], $k(x)$ is the saturated

hydraulic conductivity [LT^{-1}], k_r is the relative permeability [-] (a function of pressure head, ψ_p), S_s is the specific storage coefficient [L^{-1}], ϕ is the porosity [-], S_w is the degree of saturation [-], q_s is the general source/sink term [T^{-1}], q_e is the exchange rate with the surface [LT^{-1}] and m' is the thickness of an interface separating the surface and subsurface domains [L]. The datum is located at the ground surface ($z = 0$) with the negative z -axis pointing downward. In the current formulation, the van Genuchten (van Genuchten, 1980) relationships are used to describe the relative saturation and permeability functions.

$$S_w(\psi_p) = \frac{S_{sat} - S_{res}}{(1 + (\alpha p)^n)^{(1-1/n)}} + S_{res} \quad (7)$$

$$k_r(\psi_p) = \frac{\left(1 - \frac{(\alpha \psi_p)^{\beta-1}}{(1 + (\alpha \psi_p)^\beta)^{(1-1/\beta)}}\right)}{(1 + (\alpha \psi_p)^\beta)^{\frac{(1-1/\beta)}{2}}} \quad (8)$$

where α [L^{-1}] and β [-] are soil parameters, s_{sat} [-] is the relative saturated water content and s_{res} [-] is the relative residual saturation.

The boundary conditions are of the Neumann type

$$-k(x)k_r \nabla(\psi - z) = q_{bc} \quad (9)$$

on Γ , but can be changed to the Dirichlet type if necessary.

2.3 Exchange Flux

In previous efforts, an exchange flux q_e was used to couple the surface and the subsurface domains. It generally follows the form

$$q_e(x) = \lambda(x)(\psi_s - \psi_p) \quad (10)$$

Thus, the exchange rate depends upon the gradient across some interface and the proportionality constant $\lambda(x)$ [T^{-1}], which is a measure of the hydraulic connectivity between the two domains (Figure 1). This concept has been used extensively in studies concerned with the interactions of surface-subsurface flow and is also known as the conductance concept with λ being the conductance coefficient (Hantush, 1965; Anderson and Woessner, 1992).

Often the system of equations outlined above is solved iteratively. For example, one might iterate over q_e until some convergence criteria is fulfilled. However, since overland flow time scales may be much smaller than groundwater flow time scales, numerical instabilities often arise, necessitating adaptive time stepping and/or a fully integrated approach to solve the system of equations simultaneously (e.g., Panday and Huyakorn, 2004).

A perhaps even greater limitation of this approach lies in the assumption that there exists some distinct interface between the surface and subsurface and in the ensuing definition of the proportionality constant λ . For example, λ generally depends upon the ratio of some interface permeability k' and the interface thickness m' . It is difficult to establish evidence of such a distinct interface from direct field observations (Cardenas and Zlotnik, 2003; Kollet and Zlotnik, 2003). Additionally, often a simplifying assumption of spatial uniformity in the hydraulic interface properties is applied, because of a lack of field data. In many cases, no in-situ measurements are available and λ is used solely as a fitting parameter. The question arises, whether the conductance concept is actually a useful conceptual model of interactions between the surface and the subsurface, and implies the necessity of a more general formulation.

2.5 A general coupled surface-subsurface formulation

The previous section summarizes the current approach and points to the need for a more general formulation of the coupled surface-subsurface system. A formulation that directly couples the system of equations via the boundary condition at the ground surface is presented below. This formulation eliminates some of the problems associated with the definition of an interface conductance and numerical inefficiencies associated with the solution of the coupled system.

As shown in Figure 1, the overland flow equations may be implemented into the Richards equation at the top boundary cell under saturated conditions. Using conditions of continuity of pressure ($\psi_s = \psi_p = \psi$) and flux ($q_{bc} = q_e$) at the ground surface (Figure 1), equation (1) can be solved for for q_e

$$-q_e(x) = -\frac{\partial \|\psi, 0\|}{\partial t} + \nabla \bar{v} \|\psi, 0\| - q_r(x) \quad (11)$$

and then substituted for q_{bc} in the boundary condition in Equation (9):

$$-k(x)k_r \nabla(\psi - z) = -\frac{\partial \|\psi, 0\|}{\partial t} + \nabla \bar{v} \|\psi, 0\| - q_r(x) \quad (12)$$

where $\|A, B\|$ indicates the greater of A and B . This results in the surface water equations represented as a boundary condition to the Richards Equation. This new boundary condition is head-dependant and accounts for the movement of the free surface of ponded water at the ground surface. In Equation (12), if one assumes no lateral flow ($\nabla \bar{v} \psi = 0$) and no recharge/precipitation ($q_r(x) = 0$) the infiltration or exfiltration rate equals the vertical velocity of the free surface of ponded water. A similar formulation has been used by Neuman (1972) and Moench (1997) to account for the movement of the free water table of an unconfined aquifer.

Equation (4) now reduces to

$$S_s S_w \frac{\partial \psi_p}{\partial t} + \phi \frac{\partial S_w}{\partial t} = \nabla \cdot [k(x) k_r(\psi) \nabla(\psi - z)] + q_s \quad (13)$$

with q_e being accounted for in the new overland flow boundary condition (Equation 12), which intrinsically couples the surface and subsurface domains .

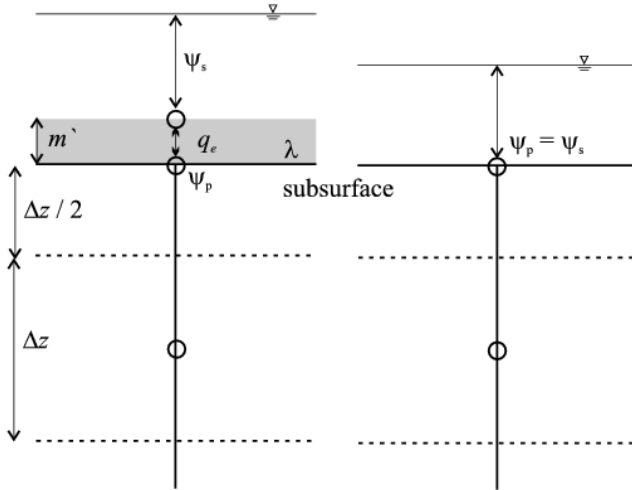


Figure 1. Schematic of the conductance concept (left) with an interface of thickness m' , which is represented by the conductance coefficient λ in theoretical models. The more general overland flow boundary is shown on the right.

2.5 Discretization and Numerical Implementation

The discretization and numerical implementation of the variable saturated groundwater flow equation has been discussed in detail (e.g. Huaykorn and Pinder, 1980). The current formulation builds upon the works of Jones and Woodard (2001) and only the details pertinent to the new overland flow boundary condition are presented here. Jones and Woodward employed an implicit backward Euler and cell-centered finite differences scheme for the discretizations in time and space, respectively. At the cell

interfaces, the harmonic averages of the saturated hydraulic conductivities and a one-point upstream weighting of the relative permeabilities are used.

For the overland flow component, a standard upwind finite control volume scheme was used for the spatial discretization and an implicit backward Euler scheme in time. The advantage of the spatial discretization methods applied in this study is that they are locally mass conservative. Discretization errors for Richards equation have been analyzed extensively by Woodward and Dawson (2000).

The solver implemented in the current study is described by Jones and Woodard (2001) and is a Newton-Krylov solution method (e.g., Saad, 2003). Newton-Krylov methods are based on a Newton linearization of the nonlinear system. The Jacobian is then solved with an iterative Krylov method. An advantage of this method is that the Krylov solver only requires matrix-vector products not the solution of the matrix itself. Additionally, Jones and Woodward (2001) preconditioned the linear system with an approximated Jacobian to improve convergence. In this study, the diagonal of the preconditioner matrix was modified to account for the overland flow boundary condition. As shown in below, this proved to be an efficient approximation of the Jacobian.

3 Numerical Simulations, Results and Discussion

No analytical solution exists for the coupled surface-subsurface system of equations presented in Section 2. This makes model verification of the coupled system problematic. The approach taken here is to verify the overland flow simulator independently and then present a series of coupled modeling examples. The overland flow simulator was verified by comparing results to an analytical solution and other overland flow models. The modeling examples presented in this section focus on the two major processes of runoff production, that are, excess saturation and excess infiltration. The influence of spatially discrete subsurface heterogeneity (in form of a low conductivity slab) on the hydrograph is studied. Additionally, we present the results from a simulation where the saturated hydraulic conductivity is represented as a space-random function using a small number of realizations. This study provides an example of the uncertainty in the simulated hydrograph due to uncertainty in subsurface heterogeneity. We conclude this section with a parallel scalability study of both the overland flow simulator and the fully coupled surface water groundwater flow model.

3.1 Model Verification

The numerical solution of the overland flow equations was verified by comparing to results published in Panday and Huyakorn (2004) and to an analytical solution. The Panday and Huyakorn results are for a two dimensional tilted V-catchment (Figure 2) for both, the gradient and critical depth outlet conditions. Additionally, Panday and Huyakorn (2004) provided results from some commonly used hydrologic simulation models, such as HSPF (Bicknell et al., 1993) and HEC-1 (USACE, 1998), the results of which are also shown here (Figure 3). The analytical solution used in the verification procedure describes a one dimensional overland flow system. Note that analytical solutions only exist for the one dimensional case.

The 2D V-Catchment Case

The problem setup for the tilted V-catchment after Panday and Huyakorn (2004) is shown in Figure 2. We simulated a 1.620km x 1km catchment slanted in the x- and y-direction with a centrally-located outlet at $800 \text{ m} \leq x \leq 820 \text{ m}$, $y=0$. The slopes of the catchment are inclined inward routing flow into the center channel. The Manning's roughness coefficients are 1.74×10^{-7} and 1.74×10^{-6} ($\text{day/m}^{1/3}$) for the slopes and the channel, respectively. An equidistant discretization of 20 m ($\Delta x = \Delta y$) was used. As described in Panday and Huyakorn (2004), for 90 minutes the rainfall rate was 3×10^{-6} m/s with a subsequent 90 minutes recession period (total simulation time of 180 minutes). A constant time step of 100 seconds was used. To compare with the other model results in Figure 3, simulations with both outlet types, gradient and critical depth, were performed.

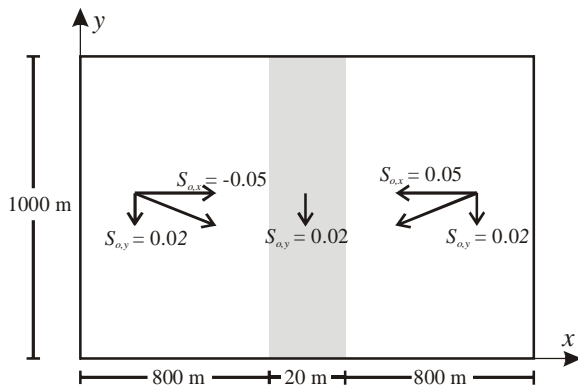


Figure 2. Plan view (not to scale) of the Problem setup of the tilted V-catchment after Panday and Huyakorn (2004).

Figure 3 shows that the ParFlow simulations for the critical depth and gradient outflow conditions are similar, because the kinematic wave approximation was used. The ParFlow simulations for the gradient outflow condition agree well with the results from MODHMS (Panday and Huyakorn) and HEC-1. The differences in model simulations, are mainly due to application of the kinematic wave approximation.

However, the differences are relatively small, because the topographic slopes are fairly large, which results in overland flow that is dominated by the gravity force (or kinematic) term.

The differences become smaller in the case of the critical depth outflow condition; due mainly to higher outflow during earlier simulation times. This results in a general decrease in the flow depth and less influence of the pressure force (or diffusive term) in the diffusive wave approximation used in e.g., MODHMS. The use of a constant time step in ParFlow that is more than an order of magnitude larger than the minimum time step of 5 seconds used in the MODHMS also contributes to differences at early simulation times. Overall the ParFlow model produces results that agree very well with other published results and lend confidence in the overland flow simulator in ParFlow. The fact that the solution method is based on the simpler kinematic wave approximation and does not explicitly distinguish between the channel and the land surface does not appear to affect the results significantly.

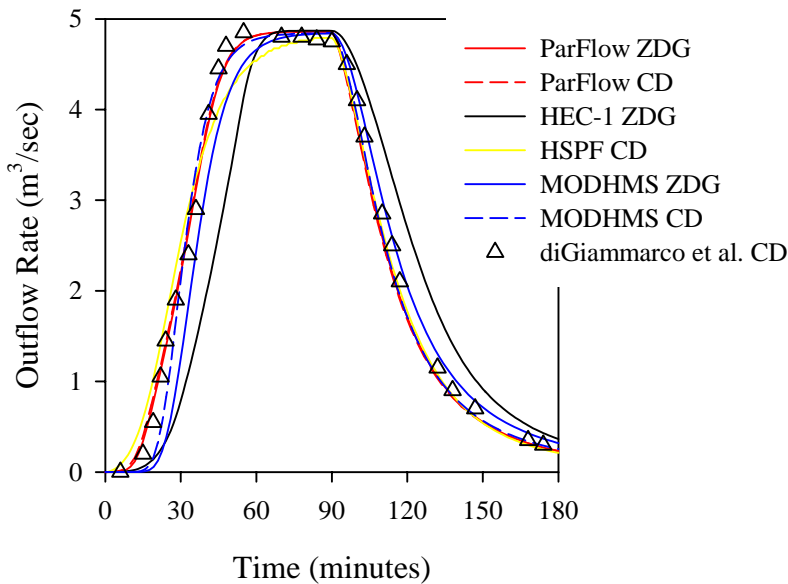


Figure 3. Comparison of simulated hydrographs for the V-catchment problem for a number of hydrologic simulation models and ParFlow.

Comparison with 1D Analytical Solution

There exist few analytical solutions for overland flow problems. The one compared to here (e.g., Gotardi and Venetulli, 1993) is for a one dimensional channel of constant slope and roughness. The parameters used in this comparison were obtained from Gotardi and Venetulli (1993) and Jaber and Mohtar (2003) and are as follows: $S_{ox} = 0.0005$, $n = 2.3 \times 10^{-7}$ (day/m^{1/3}), and $q_r = 0.33$ (mm/min). Rainfall, q_r , was applied for 200 minutes followed by 100 minutes of recession ($q_r = 0$), which resulted in 300 minutes total simulation time. The time step size was constant at 180 sec, as was the spatial discretization, $\Delta x = 80$ m. There were five cells in the x-direction ($nx = 5$) resulting in a total flow length of 400 m. The flow outlet was located at $x = 0$ and was simulated as a gradient outlet. For the remainder of the section this particular simulation is referred to as the *base case*.

Figure 4 shows the comparison between the analytical and numerical solutions. Note that the differences at the time of concentration (t_c , when the outflow equals the rainfall rate) and at the end of the recession are due to the coarse spatial resolution used in the simulation. This figure also illustrates the improvement in reproducing the analytical solution, when the lateral discretization is decreased to $\Delta x = 1$ m (increasing the spatial resolution to $nx = 400$).

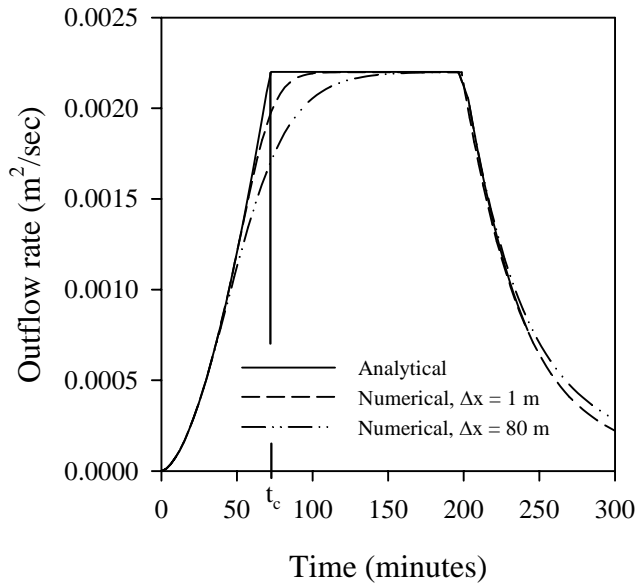


Figure 4. Comparison between the numerical (symbols) and analytical solution (solid line) for two different Δx values.

Because the accuracy (and to some extent the convergence) of the numerical solution does not directly depend on the time step size Δt , the Newton-Krylov method is very useful for solving overland flow problems, which are often fraught with numerical instabilities due to inadequate time step criteria. This is demonstrated in Figure 5, which plots the numerical solutions for a wide range of constant time step sizes. Note, that the differences in the simulated onset of the recession period are due to the coarse temporal resolution for large time steps.

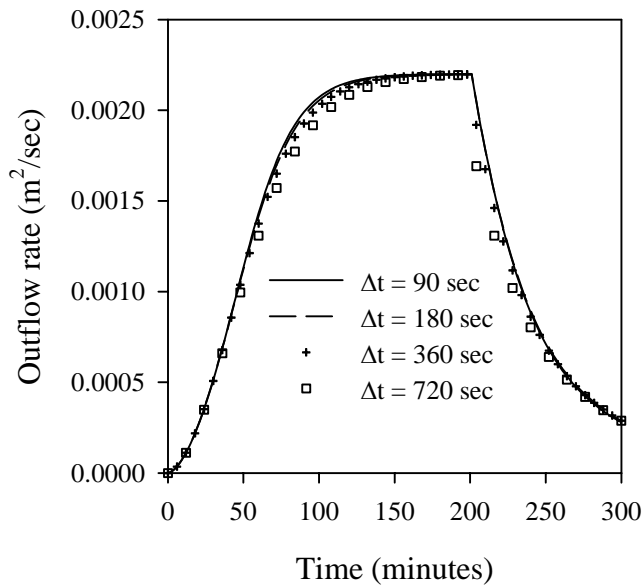


Figure 5. The effect of time step size on simulated outflow for the 1-D overland flow problem.

3.2 Integrated modeling examples

In this section we present simulations that focus on the interaction of flow between the surface and subsurface. The runoff generating processes of excess saturation and infiltration are examined and compared to the 1D *base case*. The influence of vertical spatial discretization and subsurface heterogeneity in the hydraulic conductivity on the resulting hydrograph are also investigated. In all cases the gradient outlet condition is employed and a constant rainfall rate of $q_r = 0.33$ (mm/min) is applied for 200 minutes followed by 100 minutes of recession. Table 1 provides a summary of the different simulations.

Table 1. Summary of the integrated modeling examples.

Type	WT depth (m)	Δz (m)	K_{sat} (m/day)
Excess saturation $K_{sat} > q_r$	1.0	0.2	1.0
		0.05	
	0.5	0.2	
		0.05	
Excess infiltration $K_{sat} < q_r$	1.0	0.05	0.1
		0.01	
		0.05	0.01
		0.01	
Mixed	1.0	0.05	1.0, slab: 0.01 $K_g = 0.4752$ $\sigma[\ln(K_{sat})] = 3.0$

Runoff Production by Excess Saturation, $K_{sat} > q_r$

The process of excess saturation simply involves the complete saturation of the subsurface and the intersection of the land surface by the water table, where the outcropping water table produces the runoff. To accomplish this, the hydraulic conductivity must be larger than the rainfall rate. We simulated two cases with a shallow water table located at a depth of 0.5 m and 1.0 m below the ground surface. The vanGenuchten parameters and saturated hydraulic conductivity are as follows: $K_{sat} = 1.0$ m/day, $N = 2.0$, $\alpha = 1.0$, $\theta_{res} = 0.08$, $\theta_{sat} = 0.4$. The results of these two cases are shown in Figure 6. Additionally, for each case, the sensitivity of runoff to the vertical discretization was explored. This was achieved by varying the constant vertical discretization from $\Delta z = 0.05$ m to $\Delta z = 0.2$ m. Figure 6 also shows the results from the base case for comparison. For excess saturation, Figure 6 reveals, that the vertical discretization does not have a significant impact on the predicted outflow hydrograph. This can be seen by comparing the curves using different Δz values for a given water table depth. For the water table depth of 0.5 m and 1 m, the times of ponding are some 19 minutes and 117 minutes, respectively. For the 1 m initial water table depth, no steady state is reached and the outflow rate is always smaller than rainfall rate multiplied by the length of the channel.

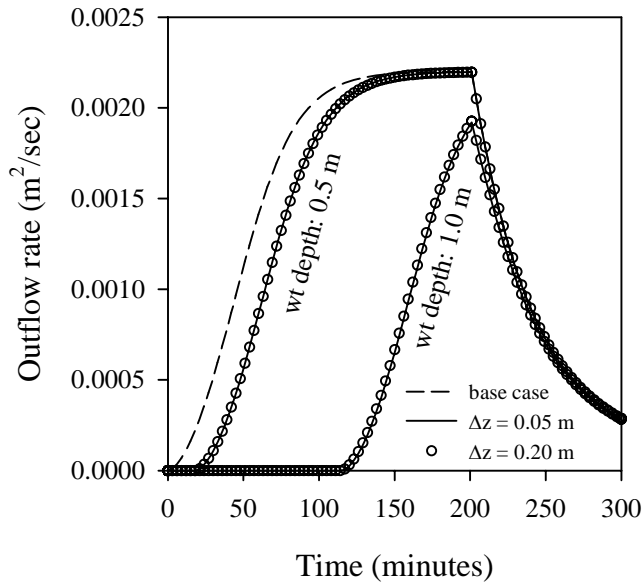


Figure 6. Comparison of the base case with simulations using $q_r < K_{sat}$ and different vertical discretizations for water table depths of 0.5 and 1.0 m.

Runoff Production by Excess Infiltration, $K_{sat} < q_r$

The more complex process of excess infiltration involves the saturation of the surface and ensuing ponding of water, before the subsurface saturates completely. For excess infiltration to occur the saturated hydraulic conductivity of the surface must be smaller than the rainfall rate.

The results of these coupled simulations are shown in Figure 7. The water table is located 1 m below the ground surface. The vanGenuchten parameters are the same as the previous set used in the excess saturation simulations. The saturated hydraulic conductivity was varied from $K_{sat} = 0.1$ to 0.01 m/day and two different vertical discretizations were used ($\Delta z = 0.05$ m and 0.01 m)

For cases where runoff is produced by excess infiltration, the vertical discretization has a significant impact on the ponding time (Figure 7). This is because the top model layer holds a finite storage volume that must be saturated for ponding to occur (e.g. Downer and Odgen, 2004). Thus, the solution becomes less accurate for large Δz values near the ground surface. This problem can be remedied by e.g., making Δz at the land surface very small.

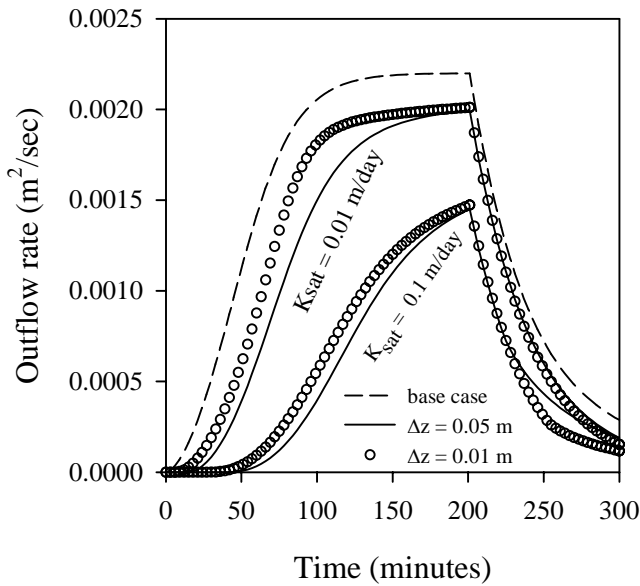


Figure 7. Comparison of the base case with simulations using $q_r > K_{sat}$ and different vertical discretizations.

Subsurface Heterogeneity in K_{sat}

A nonuniform spatial distribution of the hydraulic properties of the subsurface may have a significant impact on the observed hydrograph (Woolhiser et al., 1996). Therefore, it is important that an integrated flow model be able to account for subsurface heterogeneity. The ability of ParFlow to handle strongly heterogeneous parameter distributions has been demonstrated previously by Jones and

Woodward (2001), Tompson et al. (1999) and Maxwell et al. (2003) for subsurface flow only. The following two examples will demonstrate the usefulness of this modeling approach in simulating interactions between surface water and groundwater under heterogeneous subsurface conditions.

The first example is a variation of the excess saturation case described above. The difference is the inclusion of a 100 m long, low conductivity slab, $K_{sat} = 0.01$ m/day, located in the center of the domain extending from the land surface to a depth of 0.05m. The initial water table was set to a depth of 1.0 m below the land surface and the vertical discretization was $\Delta z = 0.05$ m. Figure 8 shows the resulting hydrograph and a comparison with the base and the homogeneous excess saturation case.

The simulated hydrograph is characterized by four distinct segments: two steep segments separated by a flat segment and a recession period after cessation of the rain (at $t=200$ minutes), which makes up the fourth segment. Figure 9 shows the temporal evolution of the flow depth distribution at the land surface. Figure 10 contains a time series of plots of the vertical relative saturation profiles of the domain starting from the initial conditions at $t = 0$. The step-like representation of the topography in ParFlow (e.g., Figure 10) is a result of the lateral discretization, the topographic slope and the finite difference grid. Figures 8 to 10 demonstrate the interactions and interdependence of excess infiltration and saturation processes in the presence of subsurface heterogeneity and are discussed in detail below.

The time series in Figure 10 ($t = 39$ min) shows that ponding first occurs in the region of the low- K_{sat} slab, because of excess infiltration. This is also illustrated by the flow depth distribution in Figure 9 at early times. The ponded water is routed over the slab and infiltrates downhill of the slab causing

saturation of the subsurface, which subsequently reaches the surface. This process causes a saturation front to form and move from the slab toward the outlet (see plots for $t = 60$ to 102 min in Figure 10).

Complete saturation of the subsurface results in the formation of a surface wave that reaches the outlet at about 110 minutes, which is reflected in the curves for $t < 110$ minutes in Figure 9. The outflow rate increases sharply as the wave arrives at the outlet (first segment of the hydrograph shown in Figure 8). At this time, the subsurface uphill from the slab is only unsaturated just below the ground surface ($t = 111$ minutes). Shortly after the entire domain becomes saturated, the hydrograph flattens, and a quasi steady state is reached for the period $135 \text{ min} < t < 150 \text{ minutes}$ (second segment). This is due to the stabilization of the flow depth profile along the slope downhill from the slab.

As soon as the subsurface is saturated completely uphill of the slab and, thus over the entire domain, a second wave is generated uphill of the slab that starts traveling toward the outlet (from $t = 117$ to 150 minutes). At 150 minutes, the outflow rate again increases sharply (third segment), when the second wave reaches the outlet ($t = 150$ to 200 minutes in Figure 8). A second steady state is not obtained in this case, because there is not enough time for the flow depth profile to stabilize over the entire domain.

After cessation of the rain at $t = 200$ minutes, the outflow rate decreases monotonically during the recession period. The subsurface beneath the slab remains partially unsaturated over the entire simulation period, though lateral redistribution of soil moisture is clearly detectable from the plots in Figure 10.

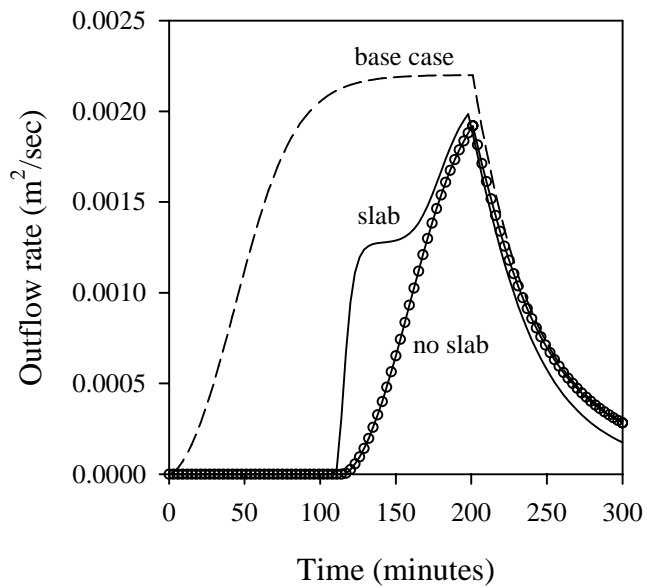


Figure 8: Plot of the outflow hydrograph as a function of time with and without a low-conductivity slab located in the center of the domain along with the base case.

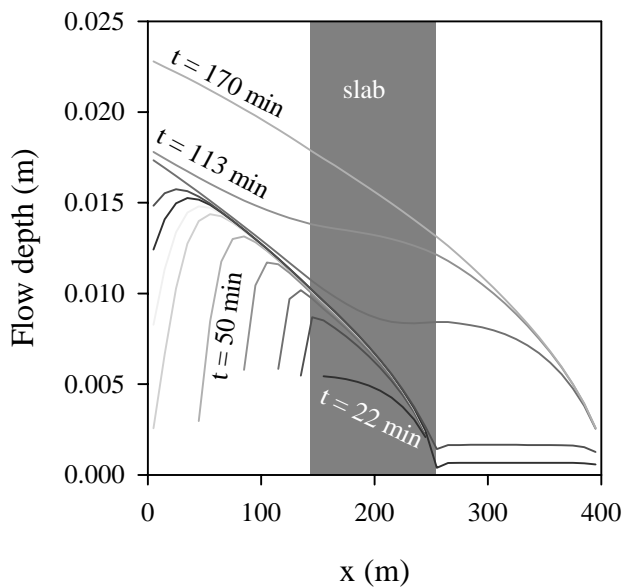


Figure 9. Plot of simulated flow depth as a function of x (lateral profiles at the land surface) for different simulation times.

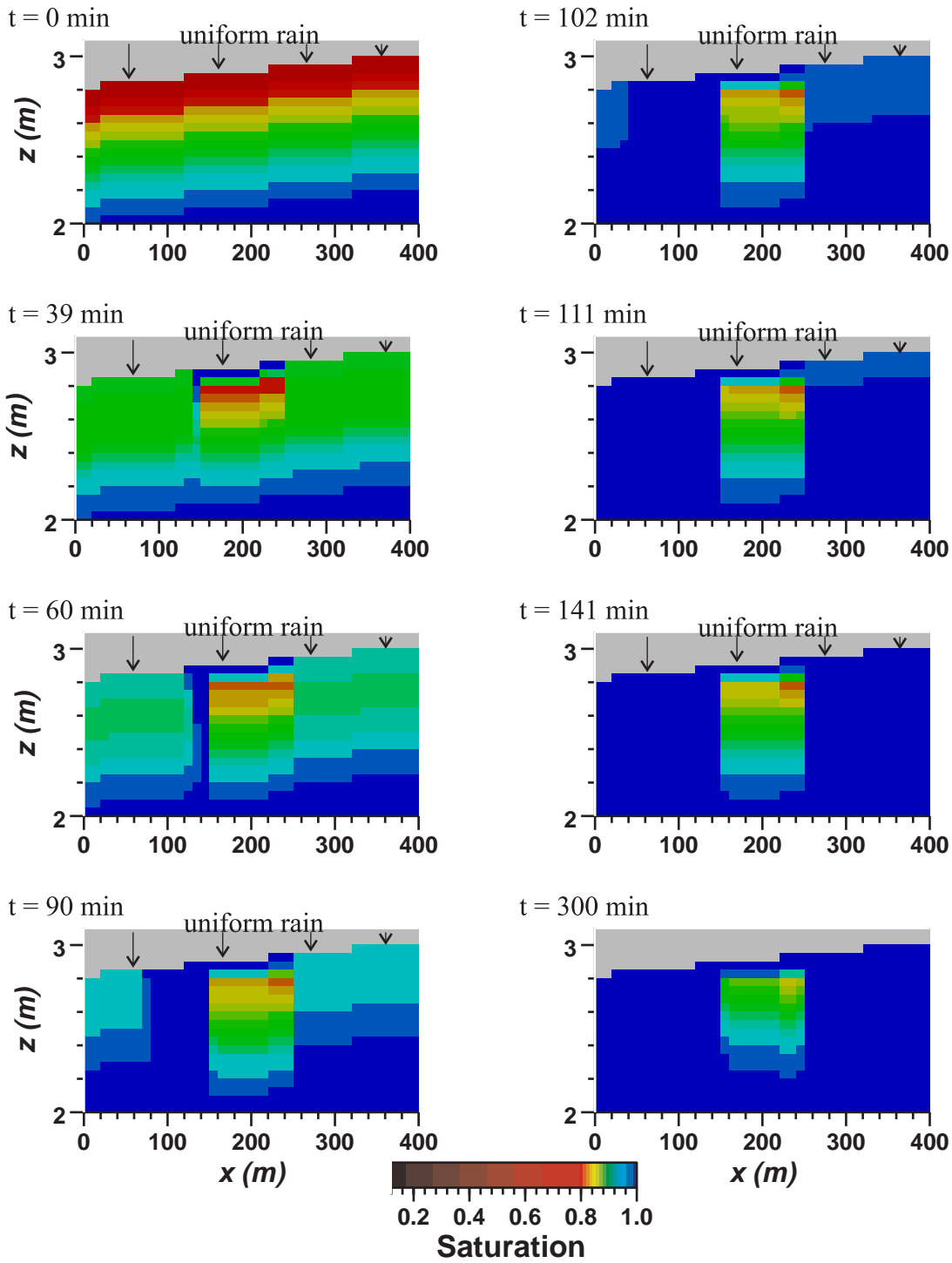


Figure 10. Snapshots of vertical profiles of relative saturation at different simulation times (note the strong vertical exaggeration).

The second heterogeneous example consists of a set of simulations, where each simulation is based on a realization of random subsurface heterogeneity in K_{sat} . We used a hypothetical, correlated Gaussian random field to describe the distribution of the saturated hydraulic conductivity (Tompson et al., 1989) with the following properties: geometric mean: $K_g = 0.4752$ m/day; standard deviation: $\sigma[\ln(k)] = 3.0$; correlation lengths in horizontal and vertical direction, respectively: $\eta_h = 50.0$ m, $\eta_z = 1.0$ m. Different random seeds were used to generate four equally likely realizations of the K_{sat} distribution. Note that the geometric mean of the distribution is equal the rainfall rate. This allows both runoff-generating processes (excess saturation and infiltration) to occur simultaneously in the simulations. The spatial distribution of these processes depends on the lateral K_{sat} distribution in the top layer of an individual realization. The initial water table depth was set at 1.0 m. The horizontal and vertical discretizations were 10 m and 0.05 m, respectively to capture the scale of the heterogeneity and the infiltration excess timing. For comparison, the model was also run for a homogeneous saturated hydraulic conductivity, $K_{sat} = K_g = 0.4752$ m/d, referred to below as the *geometric mean simulation*.

Figure 11 shows the hydrographs for four realizations of subsurface heterogeneity, the geometric mean simulation, and the base case. The spread in the curves for the different realizations is a measure of the uncertainty associated with the hydrograph due to uncertainty in the subsurface heterogeneity. Because all other parameters were kept constant and the rainfall rate was applied uniformly in space, this figure illustrates the direct impact of subsurface heterogeneity on the outflow rate. Comparing the geometric mean simulation with the different realizations, it can be seen that the geometric mean simulation underestimates the runoff rate at earlier times ($t < 150$ minutes), when the process of excess infiltration plays a dominant role in the production of runoff. For the duration $150 < t > 200$ minutes, the geometric mean simulation is bounded by the set of curves from the different realizations. During this time period

excess saturation is the main runoff-generating process. The peak outflow rate, which occurs at $t = 200$ minutes, is overestimated by the geometric mean simulation.

Another process of runoff production, which can also occur due to aquifer heterogeneity, but can be seen as being different from the processes of excess infiltration and saturation, is the formation of a perched water table that intersects the ground surface. This process of runoff production is different from excess infiltration in that it forms saturated regions in the shallow subsurface not merely the ground surface itself. A perched water table and associated runoff can only be accounted for by explicitly incorporating aquifer heterogeneity into the flow model. This runoff-generating process contributed some of the early-time runoff in the different realizations. This resulted in larger runoff rates when compared to the geometric mean simulation, which cannot account for a perched water table.

Figure 12 shows the interdependence of the different runoff generating processes due to the presence of aquifer heterogeneity for a single realization. The aquifer heterogeneity is indicated at the top, with K_{sat} varying over orders of magnitude. Inspection of the saturation profile at the bottom of Figure 12 reveals that there are regions of ponded water due to a region of low conductivity heterogeneity right at the surface and in the shallow subsurface (e.g. perched water table at around $x \cong 180$ m). The profile also exhibits an interesting feature at $x \cong 280$, where a high conductivity path conveys the ponded water from the surface directly into the deeper aquifer, highlighting the importance of aquifer heterogeneity characterization and representation in coupled surface water groundwater systems. These features also indicate the importance of subsurface heterogeneity in coupled surface-subsurface problems concerned with mass transport.

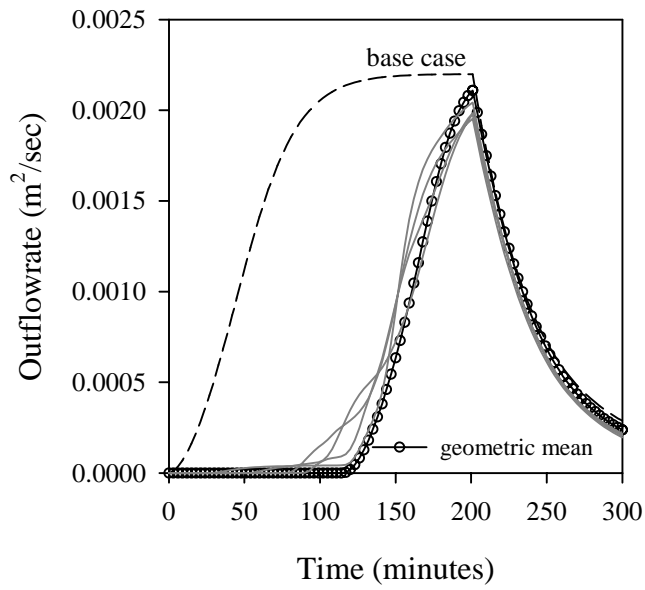


Figure 10. Results from the four Gaussian random field and geometric mean simulations. The base case is shown for comparison.

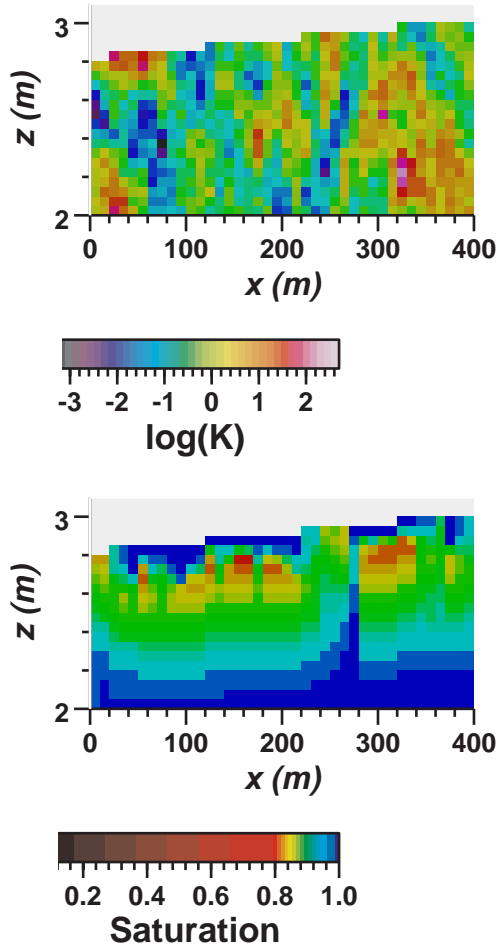


Figure 12. Example of a K_{sat} distribution of a single realization (top) and the associated relative saturation profile after 45 minutes simulation time (bottom).

Parallel Scalability

A major advantage of ParFlow over other existing integrated hydrologic modeling tools is the infrastructure devised for massively parallel computer systems (Ashby and Falgout, 1996; Jones and Woodward, 2001). The overland flow simulator discussed here is designed to exploit this infrastructure and is, thus, massively parallel as well. A determining factor of parallel efficiency is the time the code spends on inter-processor communications (communication overhead) relative to the computation time.

When the ratio between communication overhead and computation time is small, the parallel efficiency is large. Parallel efficiency of the overland flow simulator in ParFlow was studied by performing simulations of varying problem sizes and analyzing the respective run times. Following Jones and Woodard (2001) the scaled efficiency, E , is defined as $E(np,p) = T(n,1) / T(np,p)$, where T is the run time as a function of the problem size, n ; and the number of processors, p . For the case of a perfectly efficient parallel simulator, $E(np,p) = 1$, doubling the problem size and the number of processors will result in the same run time.

Figure 13 shows E for two different modeling problems: overland flow only (surface) and for the case of excess infiltration produced runoff (surface/subsurface). The two different problems were run for a smaller number of model cells (n_x, n_y, n_z) per processor (20,20,1 and 20,20,5) and for a larger number (100,100,1 and 100,100,5) to test the performance of the code for different communication overhead and computation time ratios.

For the smaller problem size, the parallel efficiency of the excess infiltration case is significantly higher than for the overland flow only case. The scaled efficiency for the excess infiltration case levels off at about 0.60, whereas the scaled efficiency for the overland flow only case levels off at about 0.45. This is due to relatively small computational times at individual processors for the overland flow only case and, thus, large communication overhead versus computation time ratios.

This trend, however, is reversed when the problem size at each processor is increased to 100,100,1 and 100,100,5. Figure 13 shows a significant increase in the scaled efficiency for the overland flow only case, which now levels off at about 0.82. An increase, though smaller, is also observed in the saturation

excess case, which now levels off at 0.72. This is due to larger increases in the computation time compared to the communication overhead and results in a smaller communication overhead versus computation time ratio demonstrating the parallel efficiency of ParFlow.

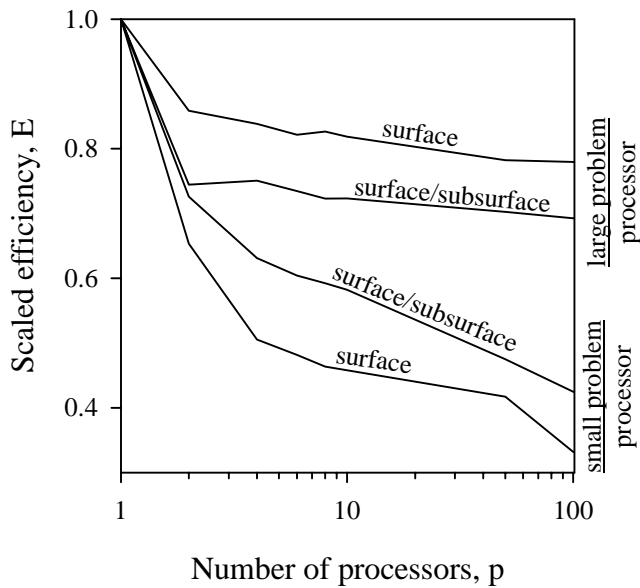


Figure 13. Scaled parallel efficiency for simulations of surface flow only and surface/subsurface flow using small and large problem sizes per processor.

4 Conclusions

A new formulation of coupled surface water groundwater flow, which does not depend on a conductance-like relationship, has been described. This formulation forms the basis of an overland flow simulator based on the kinematic wave approximation, that has been implemented in the parallel, three-dimensional, variable saturated flow code ParFlow. The overland flow simulator takes the form of a free-surface upper boundary condition for the problem of variable saturated groundwater flow and is therefore fully integrated.

The overland flow simulator was verified using previously published data and an analytical solution. The globalized Newton solution methods allow for the application of very large time steps without compromising numerical stability, which is an advantage over other approaches that are based on restricting stability criteria. Simulation examples were presented that focused on the two main processes of runoff production, excess saturation and infiltration. The effect of varying vertical discretization was also studied. Changes in the vertical discretization had a significant impact on the solution only in the case of excess infiltration, due to dependence of the time of ponding on the finite storage of the top layer.

We have shown that shallow subsurface heterogeneity may have a strong influence on the outflow rate and may cause a segmented hydrograph. A set of simulations where a heterogeneous subsurface was simulated as a correlated random field was used to demonstrate how uncertainty due to subsurface heterogeneity influences uncertainty in runoff predictions. A comparison with a homogeneous geometric mean simulation of the hydraulic conductivity showed that the geometric mean simulation may not account for excess infiltration and thus underestimates early parts of the hydrograph. Because

the new coupled formulation can explicitly account for subsurface heterogeneity, the production of runoff due to the formation of a perched water table can be simulated. This process of runoff production is generally neglected by other hydrologic modeling tools and acts on a time scale between excess infiltration (short time scale) and excess saturation (long to very long time scale) depending on the depth of the water table from the ground surface.

A parallel efficiency study showed the excellent scalability of the overland flow simulator and the fully-coupled surface-subsurface simulator for large problems. This makes this new coupled model especially suitable for small and large watershed modeling, where the efficient use of large computational resources is vital.

5 Acknowledgements

This work was conducted under the auspices of the U. S. Department of Energy by the University of California, Lawrence Livermore National Laboratory (LLNL) under contract W-7405-Eng-48. This work was funded by DOE Fossil Energy Program NETL, NPTO, Tulsa, OK and by the LLNL OPC program. We are especially indebted to S. Panday for providing the original data for Figure 3 and Andrew Tompson for the constructive discussions.

5 References

- Anderson MP, Woessner WW. Applied groundwater modeling: simulation of flow and advective transport. Academic Press, San Diego 1992; p. 281.
- Ashby SF, Falgout RD. A parallel multigrid preconditioned conjugate gradient algorithm for groundwater flow simulations. Nucl Sci Eng 1996;124(1):145-59.
- Bicknell BR, Imhoff JL, Kittle JL, Donigian AS, Johanson RC. Hydrologic Simulation Program FORTAN (HSPF): User's Manual for Release 10, EPA-600/R-93/174, US Environmental Protection Agency, Athens, GA, 1996.
- Braunschweig, F., P.C. Leitao, L. Fernandes, P.Pina and R.J.J. Neves. The object-oriented design of the integrated water modelling system MOHID. Proceedings of the XV International Conference on Computation Methods in Water Resources (CMWR XV), Chapel Hill, NC, USA, Elsevier, 2004; 2:1079-90.
- Cardenas MBR, Zlontik VA. Three-dimensional model of modern channel bend deposits. Water Resour Res 2003;39(6),1141,doi:10.1029/2002WR001383.
- Downer CW, Odgen FL. Appropriate vertical discretization of Richards' equation for two-dimensional watershed-scale modeling. Hydrol. Process. 2004;18:1-22.
- Fiedler FR, Ramirez JA. A numerical method for simulating discontinuous shallow flow over an infiltrating surface. Int J Numer Meth Fluids 2000;32:219-40.
- Forsyth PA, Wu YS, Pruess K. Robust numerical methods for saturated-unsaturated flow with dry conditions in heterogeneous media. Adv. Water Resour 1995;18:25-38.
- Freeze, R.A. and R.L. Harlan. Blue-print for a physically-based digitally simulated hydrologic response model. J Hydrol. 1960; 9, 237-58.

- Gottardi G, Venutelli M. A control-volume finite element model for two dimensional overland flow. *Adv Water Resour* 1993;16:227-84.
- Govindaraju RS and Kavvas ML. Dynamics of moving boundary overland flows over infiltrating surfaces at hillslopes *Water Resour Res* 1991; 27(8), 1885-98.
- Gunduz O and Mustafa MA. River networks and groundwater flow: a simultaneous solution of acoupled system. *J Hydrol* 2005;301:216-34.
- Hantush MS. Wells near streams with semipervious beds. *J Geophys Res* 1965;70:2829-38.
- Huyakorn PS, Springer EP, Guvanasen V, Wadsworth TD. A three dimensional finite element model for simulating water flow in variable saturated porous media. *Water Resour Res* 1986;22(12):1790-808.
- Huyakorn, P. S. and G.F. Pinder, *Computational Methods In Subsurface Flow*, New York: Academic Press, 1983.
- Jaber FH, Mohtar RH. Stability and accuracy of two-dimensional kinematic wave overland flow modeling. *Adv Water Resour* 2003;26;1189-98.
- Jones JE, Woodward CS. Newton-Krylov-multigrid solvers for large-scale, highly heterogeneous, variable saturated flow problems. *Adv Water Resour* 2001;24:763-74.
- Jones JE, Woodward CS. Preconditioning Newton-Krylov methods for baribale saturated flow. In: Bentley LR, Sykes JF, Brebbia CA, Gray WG, Pinder GF, editors. *Computational methods in water resources*, vol. 1. Balkema: Rotterdam; 2000. p. 101-6.
- Kirkland MR, Hills RG, Wierenga PJ. Algorithms for solving Richards' equation for nonuniform porous media. *Water Resour Res* 1992; 28:2049-58.
- Kollet SJ, Zlontik VA. Stream depletion predictions using pumping test data from a heterogeneous stream-aquifer system (a case study from the Great Plains, USA). *J Hydrol* 2003;281:96-114.

- Kutilek M, Nielsen DR. Soil Hydrology. Cremlingen-Destedt: Catena –Verl 1994: 370.
- Kutilek M, Nielson DR. Soil hydrology. GeoEcology, Catena Verlag, Cremlingen-Destedt, Germany, 1994; p. 370.
- LaBolle EM, Ahmed AA, Fogg GE. Review of integrated groundwater and surface water model (IGSM). Ground Water 2003;41(2):238-46.
- Maxwell RM, Welty C, Tompson AFB. Streamline-based simulation of virus transport resulting from long term artificial recharge in a heterogeneous aquifer. Adv Water Resour 2003;25(10):1075-96.
- Miller CT, Williams GA, Kelley CT, Tocci MD. Robust solution of Richards' equation for nonuniform porous media. Water Resour Res 1998;34:2599-610.
- Moench, A. Flow to a well of finite diameter in a homogeneous, anisotropic water table aquifer. Water Resour Res 1997;33(6):1397-407.
- Neuman SP. Theory of flow in unconfined aquifers considering delayed aquifer response. Water Resour Res 1972;8(4):1031-44.
- Panday S, Huyakorn PS. A fully coupled physically-based spatially-distributed model for evaluating surface/subsurface flow. Adv Water Resour 2004;27:361-82.
- Putti, M and C. Paniconi. Time step and stability control for a coupled model of surface and subsurface flow. Proceedings of the XV International Conference on Computation Methods in Water Resources (CMWR XV), Chapel Hill, NC, USA, Elsevier, 2004; 2:1391-1402.
- Saad Y. Iterative methods for sparse linear systems. 2nd edition, SIAM, Philadelphia, 2003.
- Taylor C, Al-Mashidani G, Davis JM. A finite element approach to watershed runoff. J Hydrol 1974;21:231-46.

- Therrien R, Sudicky EA. Three-dimensional analysis of variable-saturated flow and solute transport in discretely-fractured porous media. *J. Contam. Hydrol.* 1996;23:1-44.
- Tompson, A.F.B., R. Ababou, and L. Gelhar. Implementation of the 3-dimensional turning bands random field generator, *Water Resour. Res.*, 1989; 25(10), 2227-43.
- Tompson AFB, Carle SF, Rosenberg ND, Maxwell RM. Analysis of groundwater migration from artificial recharge in a large urban aquifer: A simulation perspective. *Water Resour Res* 1999;35(10):2981-98.
- USACE. HEC-1: Flood Hydrograph Package, User's Manual, Version 4.1, US Army Corps of Engineers, Hydrologic Engineering Center, Davis, CA, 1998.
- Van Genuchten MTh. A closed-form equation for predicting the hydraulic conductivity of unsaturated soils. *Soil Sci SocAm J* 1980;44:892-98.
- VanderKwaak JE. Loague K. Hydrologic-response simulations for the R-5 catchment with a comprehensive physics-based model. *Water Resour Res* 2001;37(4):999-1013.
- Wallach R, Grigorin G, Rivlin(Byk) J. The errors in surface runoff prediction by neglecting the relationship between infiltration and overland flow depth. *J Hydrol* 1997;200:243-59.
- Woodward CS, Dawson CN. Analysis of expanded mixed finite element methods for a nonlinear parabolic equation modeling flow into variable saturated porous media. *SIAM J Numer Anal* 2000;37(3):701-24.
- Woolhiser DA, Smith RE, Giraldez JV. Effects of spatial variability of the saturated conductivity on Hortonian overland flow. *Water Resour Res* 1996;32(3):671-78.